Technical Sciences
Academy of Romania
www.jesi.astr.ro

*Journal of Engineering Sciences and Innovation*
*Volume 2, Issue 2 / 2017, pp. 58-74*

***D. Chemical Engineering, Materials Science and Engineering, Natural Resources***

# The determination of the gradient and thermal stresses for the heating of type 18-10 stainless steel ingots

**IOAN ILCA***

*University Politehnica Timişoara, Faculty of Engineering Hunedoara, Revoluţiei 5, Hunedoara, Romania*

**Abstract**: The aim of this paper is to determine the gradient and thermal stresses depending on the heating rates, based on parameters resulted from industrial studies, for the purpose of optimizing the heating of type 18-10 stainless steel ingots, considering the cases where the heating is required starting from the cold state. If the heating for the plastic deformation processing is to begin from the cold state, the determination of the heating rate up to the temperature of 700 – 800 ºC must be done with extreme care, as this is in fact the most conducive period to the formation of defects. Having analysed the existing domestic and foreign situation, the heating process for this type of steel raises difficult issues and differs from one company to another, relying mostly on their own accumulated experience. Despite the fact that, practically, the possibility of increasing the heating rate has been demonstrated, it is restrained by the fear of achieving an insufficient section heating and of the destruction of steel's tightness during the initial heating period. For these reasons we have taken the step of the analytical review of the gradient variation, as well as of the thermal stresses during the preheating period.

**Keywords:** steel ingot, thermal gradient, thermal stresses, heating rate.

## 1. Introduction

During the process of hot-metal working by rolling or forging, the heating of ingots has a decisive influence on the quality of products. When selecting the heating method one must take into consideration the properties of the steel and the type of their subsequent processing.

Therefore, the heating of stainless-steel ingots requires a greater caution and attention than the heating of semi-manufactured products, which can be explained by the characteristics of the structure and properties of the cast metallic material, more prone to the formation of defects during the hot-metal working process [1,2].

* Correspondence address: ilca@fih.upt.ro

The factors which determine the influence of the heating over the quality are: the temperature and heating uniformity, the heating rate and the condition of the furnace's atmosphere [3].
The analysis of these factors reveals that the heating temperature and uniformity are decisive factors and maybe even more important than the rate or duration of the heating [4].
The matter of the influence of the heating regimen takes on considerable importance for steels with high carbon content and for alloy steels. Because of the characteristics of the structure, their heating technology is more complicated and requires a greater responsibility than in case of mild steels and steels with average carbon content.
Indeed, steels with high carbon content and alloy steels do possess a series of characteristics that hinder and delay the heating processes, seeing that [5,6,7]:

- they have smaller heat-transfer coefficients;
- they are more sensitive to the factors affecting quality by overheating and burning, occurrence of thermal stresses and formation of cracks;
- during processing, they are more resistant to deformation and, as a consequence, have smaller optimal plasticity ranges, requiring a greater heating uniformity on the entire volume of metallic material.

The paper aims to compare practical data obtained from industrial research with theoretical calculation methods with a view to their approximation.

## 2. Content

The cracking of stainless steel ingots during heating is caused by thermal stresses whose value becomes comparable with the endurance limit before their core temperature exceeds their perfect elasticity (500 – 550 ºC) [8,9,10].
If the temperature variation inside the body of the ingot can be determined experimentally, thermal stresses can only be evaluated analytically [11].
The analytical determination of thermal stresses is based on the relations in the theory of elasticity: for this reason, when solving the heat transmission equations using the basic principles of the theory of elasticity, we obtain results which do not correspond to a sufficient degree with the practical data. These results can be considered to be only a first approximation which requires correction with the help of experimental data [12, 13].
The innovations that we bring with this paper includes researching the temperature gradient variation at different speeds in heating ovens (furnaces flame deep inverted) for 3,6t cold ingot steel.
On this basis, it determines the radial thermal stresses that can generate cracks, if the value exceeds the tensile strength of the steel, respectively.
For the purpose of measuring the temperature inside an austenitic stainless steel ingot (type 18-10, i.e. 18% Cr and 10% Ni) stabilized with Mo and Ti, three

orifices for Rh-RhPt thermocouples were drilled until the central axis, laid out in the same cross section (Fig. 1). The experiments were conducted at the ArcelorMittal S.A. company in Hunedoara.

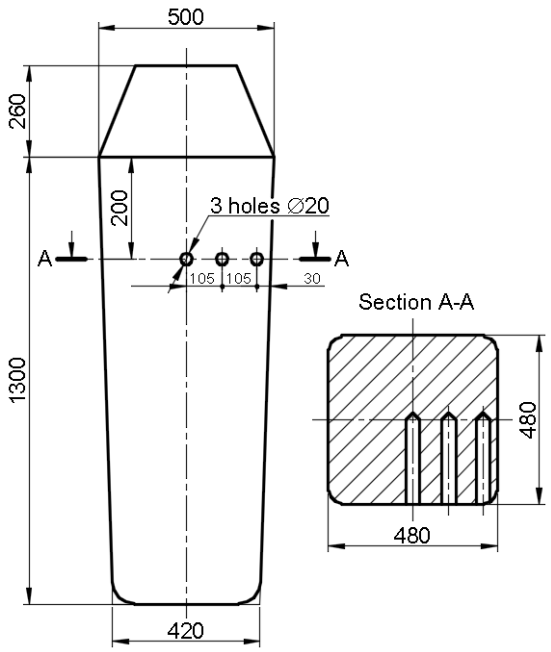


Fig. 1. Lay-out of thermocouples for measuring the temperature inside an experimental ingot.

In order to have a criterion for comparison regarding the manner in which the heating rate influences the value of the thermal gradient, experiments for reproducing the previously recorded diagram when heating a batch of austenitic stainless steel using the existing technology were conducted under industrial conditions.

As it can be observed from Figure 2, with the exception of the first 0.5 h period, the furnace temperature followed the described process (with the exception of the equalization period), resulting in a maximum temperature difference between the centre and the surface of the ingot of 130ºC, 1.5 h after charging the ingot into the furnace. Next, even though the furnace temperature begins to rise with a mean rate of 50ºC/h, the temperature difference is maintained at around 100ºC until the start of the homogenization period at 900ºC, period that lasts for 3 hours. The same diagram shows the variation in time of the ingot's temperature when air cooled, after the end of the homogenization period at 900ºC.

The value of the gradient obtained from cooling down from this temperature is somewhat diminished by the influence of the furnace hearth, which, being hot, constituted a source of heat whose effect could not be neglected. Nevertheless, the

maximum temperature difference of 170 ºC is obtained after approximately 0.5 hours and it must be considered as being smaller than in case of cooling down from the recommended rolling temperature for this steel.

This shows that the gradient can reach values that may cause the formation of cracks not only during the preheating period, but especially after removal from the furnace and rolling between cooled cylinders, when the intense temperature loss from a thin layer at the surface of the ingot cannot be compensated by the inner heat because of the low thermal conductibility of this steel.

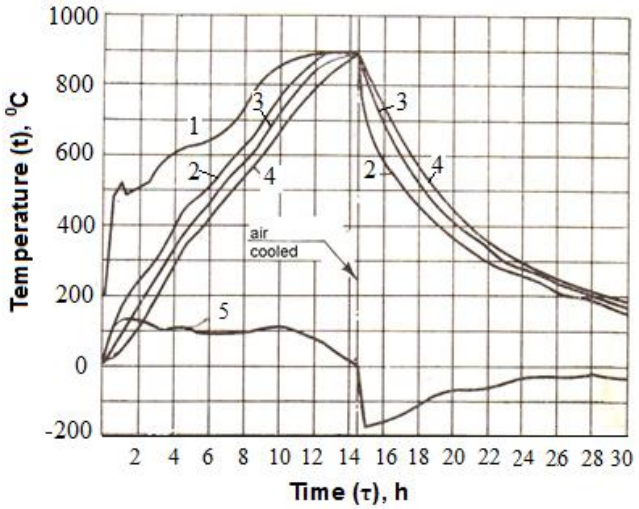


Fig. 2. Heating the austenitic stainless steel ingot up to the homogenization temperature, by reproducing the diagram of practical heating under industrial conditions and air cooling: 1 – furnace temperature; 2 – temperature at the surface of the ingot; 3 – temperature in midline section; 4 – temperature at the centre of the ingot; 5 – temperature gradient.

In the next two variants (Fig. 3, a and b), the experimental ingot was charged into the furnace heated at different temperatures (400ºC, 500ºC respectively) and, without a prior holding, the heating process was guided at steps of 51ºC/h, and in the second case, of 79ºC/h.

In both variants, the value of the gradient increases but, in the second variant (Fig. 3 b), the maximum value of 210ºC is almost double than the value obtained when the holding was performed at 500ºC. The experimented variants (Fig. 4 and 5) explored the variation of the gradient at different heating rates, while observing the holding period.

The ingot was charged in the furnace heated at approximately 530ºC and, after a holding period of 2 and 2.5 hours, the temperature of the furnace was increased with 30ºC/h, and 71ºC/h respectively, the latter variant in order to be compared with the case where the heating of the ingot is performed with approximately the same rate (Fig. 3b), but without the holding period.

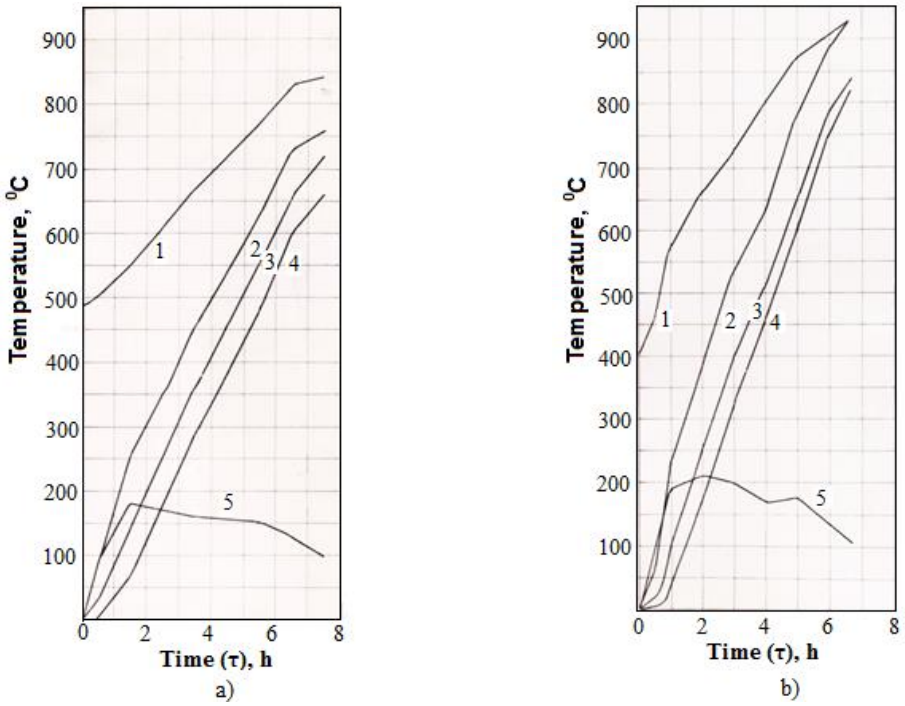


Fig. 3. Temperature evolution in the heating process of the 18-10 type steel ingot at a low rate of 51 ºC/h (Fig. 3 a) and at a high rate of 79 ºC/h (Fig. 3 b), without holding in the initial period: 1 – furnace temperature; 2 – temperature at the surface of the ingot; 3 – temperature in midline section; 4 – temperature at the centre of the ingot; 5 – temperature difference between the surface and the centre of the ingot.

The higher value of the maximum 160ºC gradient in the variant illustrated in Figure 5, in comparison with the other variants where an appropriate holding at heat was performed, can be explained by the sudden increase of the temperature inside the furnace to 590ºC, slightly before reaching the maximum value, impressing a more rapid heating on the surface of the ingot.

When comparing the variants illustrated in Figures 5 and 3a, with and without holding at heat, one can observe that after 7.5 hours, the ingot has approximately the same temperature, but the maximum gradient, even in the situation mentioned before, is 20ºC lower if the holding at heat was performed.

At comparable heating rates, 71ºC/h (Fig. 5) and 79ºC/h (Fig. 3b) the differences are obvious.

Two of the presented variants have simulated the heating of ingots after being charged into the furnace in a hot state. After a cooling period of 3 hours in the furnace (Fig. 4) and after air cooling (Fig. 5) when the temperature at the centre of the ingot returned to 500 – 520ºC, the heating process was resumed at a heating rate of 114ºC/h and 207ºC respectively. We can observe that when reheating, the gradient subsides after 0.6 – 0.7 h, but reaches its peak at time intervals inversely proportional to the heating rates.

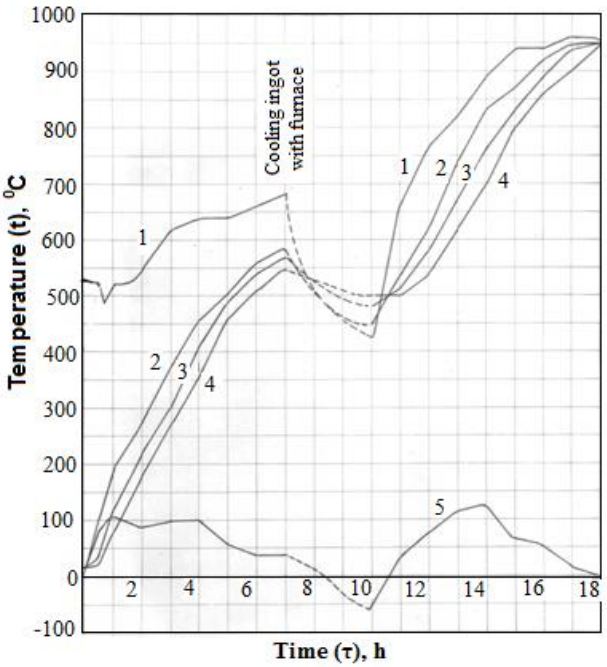


Fig. 4. Temperature evolution when the experimental ingot is heated with an initial holding at heat period, at low heating rate and the simulation of ingot heating when charged into the furnace in warm state: 1 – furnace temperature; 2 – temperature at the surface of the ingot; 3 – temperature in midline section; 4 – temperature at the centre of the ingot;
5 – temperature difference between the surface and the centre of the ingot.

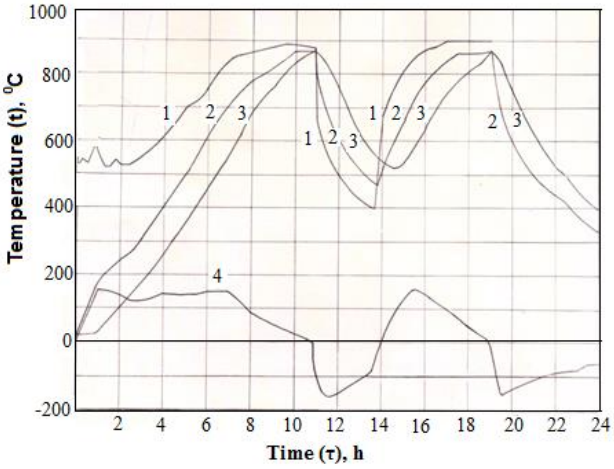


Fig. 5. Temperature evolution when the experimental ingot is heated with an initial holding period, at an increased heating rate and the simulation of ingot heating when charged into the furnace in warm state: 1 – furnace temperature; 2 – temperature at the surface of the ingot; 3 – temperature at the centre of the ingot; 4 – temperature difference on section.

Despite the substantial differences between the heating rates, the maximum gradient increases with only 30ºC, which is an indication of a strong improvement in the thermal conductibility of the steel if the temperature at the centre of the ingot exceeds 500ºC.

After homogenization at 900ºC the steel was then air cooled, which allowed for the gradient variation to be determined under these conditions as well (Fig. 2 and 5). The experimented variants show that lower values of the gradient concomitantly with a shortening of the heating time are obtained by maintaining the furnace temperature at a constant value (~ 500 – 600ºC), after the cold ingots are charged.

In this case one can observe that the duration for obtaining the maximum gradient value is of approx. 1 h (Fig. 2, 4 and 5), compared to 1,5 – 2 h (Fig. 3, a and b) when the holding at heat period was eliminated.

In both variants, the gradient begins to decrease when the temperature at the centre of the ingot increases. Therefore, it is a practical necessity for the heating of cold ingots of this quality to establish the holding period at the furnace temperature of maximum 2 h, with the guarantee that the exceedance of the moment of maximum gradient, close to the critical value, is ensured.

The heating rate which is then applied until reaching the temperature of approx. 550ºC at the centre of the ingot is only limited by the value of the critical gradient.

The determination by way of experiment of the critical gradient's value is a difficult task, given that large temperature differences on section can cause the formation of micro-cracks in the body of the ingots even before the formation of surface cracks. These are accentuated during plastic deformation and most of the times lead to the destruction of the semi-manufactured product and to an increase in metal consumption.

For these reasons, we have taken the step of the analytical review of the gradient variation, as well as of the determination of thermal stresses during the preheating period.

Thus, Figure 6 shows the analytical review of the temperature evolution at the centre and surface of the ingot and the determination of the thermal stresses for the variant illustrated in Figure 2, taking as a basis the solutions of differential equations of Fourier's law of heat conduction.

Seeing that the practical application of mathematical solutions is complicated because of the fact that, in addition to coordinates and time, the thermal field is influenced by other measures as well, such as: temperature dependent physical constants, the sizes of the volume subjected to heating, etc., the solutions were presented in terms of the complex nondirectional values of criteria and simplexes (the Fourier criterion $\frac{a\tau}{R^2}$, simplexes $\frac{\alpha R}{\lambda}; \frac{r}{R}$), which allow for the reduction of the number of variables and ease their application in practice. The placing of temperature measurement points has allowed the experimental ingot to be considered of infinite length and, as a simplification, it was considered to have a cylindrical shape, with a radius equivalent to $R = \frac{\sqrt{L^2}}{\pi}$, while the heating was carried out axially symmetrical.

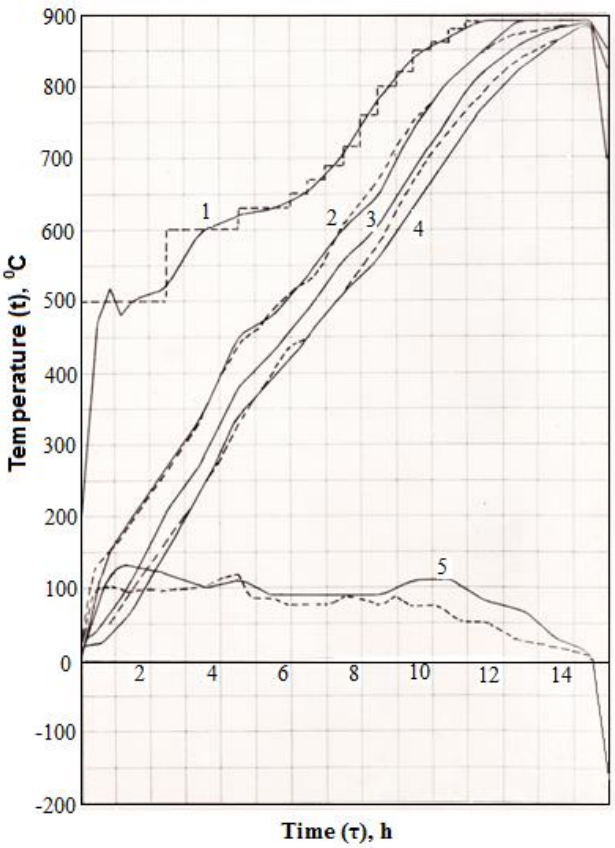


Fig. 6. Comparison between the experimental curves and the curves determined analytically when heating the 18-10 type stainless steel ingot experimental curves;
---------- analytically determined curves.
1 – furnace temperature; 2 – temperature at the surface of the ingot; 3 – temperature in midline section; 4 – temperature at the centre of the ingot; 5 – temperature difference between the surface and the centre of the ingot.

Explanations of computations:

$\lambda$ – thermal conductivity coefficient, $(W/mK)10^{-3}$; $C_p$ – heat capacity, J/kg K; $\gamma$ – weight capacity, $kg/m^3$; E-elastic modulus, $daN/mm^2$; $\beta$ – linear dilatation coefficient, $^oC^{-1}$; $\nu$ - Poisson's coefficient (for steel = 0.3); $a = \frac{\lambda}{C_p \gamma}$ – temperature diffusivity coefficient, $m^2/h$; $\tau$ = time, h; ts = ingot surface temperature, $^oC$; $\Delta t_m$ – maximum temperature gradient on section, $^oC$; R – ingot radius approximated to a cylinder, m; r – distance from ingot axis to its surface, m; $v_i$ – heating speed, $^oC$; L – ingot's width, m; $t_c$ - ingot's centre temperature, $^oC$; $\alpha$ – global heat transfer coefficient, $W/m^2K$; $h = \frac{\alpha}{\lambda}$ – relative heat transfer coefficient, $m^{-1}$.

The temperature at the surface and at the centre of the ingot was calculated at 0.5 h intervals. It was considered that the ingot's temperature when charged into the furnace was $t_o$, and the furnace's temperature $t_a$.
The section distribution after the first heating period is described by the equation:

$$t = t_a + (t_0 - t_a)\sum_{n=1}^{\infty} \frac{2I_1(\mu_n)}{\mu_n[I_0^2(\mu_n)+I_1^2(\mu_n)]} \cdot I_0\left(\mu_n \frac{r}{R}\right) e^{-\mu_n^2 \cdot \frac{a\tau}{R^2}} \quad (1)$$

which, taking into account the fact that the roots of the Bessel functions depend on the $\frac{\alpha R}{\lambda}$ relation, can be transcribed in a simplified form:

$$\frac{t - t_a}{t_0 - t_a} = \Phi\left(\frac{a\tau}{R^2}; \frac{\alpha R}{\lambda}; \frac{r}{R}\right) \quad (2)$$

In the next stages, the occurrence of a thermal gradient imposes the modification of the equation (1) by adding the term which takes into account heat distribution on the ingot's section:

$$\begin{aligned} t = t_a + (t_0 - t_a)\sum_{n=1}^{\infty} \frac{2I_1(\mu_n)}{\mu_n[I_0^2(\mu_n)+I_1^2(\mu_n)]} \cdot I_0\left(\mu_n \frac{r}{R}\right) e^{-\mu_n^2 \cdot \frac{a\tau}{R^2}} - \\ - \Delta t_0 \sum_{n=1}^{\infty} \frac{4I_2(\mu_n)}{\mu_n^2[I_0^2(\mu_n)+I_1^2(\mu_n)]} \cdot I_0\left(\mu_n \frac{r}{R}\right) e^{-\mu_n^2 \cdot \frac{a\tau}{R^2}} \end{aligned} \quad (3)$$

which, for the same reasons, can be transcribed as:

$$t = t_a + (t_0 - t_a)\Phi_n - \Delta t_0 \Phi_{n1} \quad (4)$$

seeing that from the computations results: $\Phi_{n1} = 0.6\Phi_n$ then

$$t = t_a + (t_0 - t_a - 0.6\Delta t_0)\Phi_n \quad (5)$$

Using the graphic representation of the $\Phi_n$ functions, with the help of the (2) and (5) relations, the ingot's temperature for $\frac{r}{R} = 1$ and $\frac{r}{R} = 0$ was calculated.
The temperature dependant variation of the parameters involved in the computation is shown in Table 1.

Table 1. Value of the employed coefficients depending on the temperature

| **$t^0$C** | **0** | **100** | **200** | **300** | **400** | **500** |
|---|---|---|---|---|---|---|
| λ [W/mk10$^{-3}$] | 15.9 | 16.3 | 17.2 | 18.4 | 20.1 | 21.7 |
| γ [10$^3$Kg/m$^3$] | 7.92 | 7.98 | 7.84 | 7.80 | 7.75 | 7.71 |
| $c_p$ [J/kgK] | - | 0.502 | 0.511 | 0.523 | 0.527 | 0.536 |
| E [10$^3$N/mm$^2$] | 196.2 | 190.0 | 180.5 | 175.0 | 156.9 | 151.1 |
| β x10$^{-6}$[C$^{-1}$] | - | 14.8 | 16.5 | 17.1 | 17.6 | 18.0 |

| **$t^0$C** | **600** | **700** | **800** | **900** | **1000** |
|---|---|---|---|---|---|
| λ [W/mk10$^{-3}$] | 23.8 | 25.6 | 26.7 | 26.7 | 28.0 |
| γ [10$^3$Kg/m$^3$] | 7.66 | 7.66 | 7.56 | 7.51 | 7.46 |
| $c_p$ [J/kgK] | 0.544 | 0.548 | 0.557 | 0.561 | 0.561 |
| E [10$^3$N/mm$^2$] | 145.2 | – | 126.5 | – | – |
| β x10$^{-6}$[C$^{-1}$] | 18.4 | 18.8 | 19.0 | 19.2 | 19.4 |

As one can observe from Figure 6, the calculated values (the curves shown in dotted line), especially at low temperatures, are close to the experimental ones.
The axial thermal stresses which occur during the heating process until the moment when the temperature at the centre of the ingot reaches 550ºC, a point when the metallic material is considered to have a sufficient plasticity and they subside, has been analytically determined for the same variant.
The computation was performed using three methods considered by the author more appropriate for practical situations, using relations from the theory of heat transfer in steel ingots [14,15,16,17]:

- the furnace temperature is changed in increments;
- linear modification of the temperature on the surface of the ingot;
- heating at different rates (real diagram).

The method of determining the stresses resulted from heating for each of these methods is analysed.
For the first method, the most frequent case in industrial practice, the value of stresses with and without the existence of an initial thermal gradient, is given by the relation (6):

$$\sigma_z = \frac{\beta E}{1-\upsilon}\cdot\frac{v_i\cdot R^2}{8a}\left(1-2\frac{r^2}{R^2}\right)+\frac{\beta E}{1-\upsilon}\cdot\frac{R^2}{a}\sum_{n=1}^{\infty}\frac{2}{\mu_n^4}-\mu_n\frac{I_0\left(\mu_n\cdot\frac{r}{R}\right)}{I_1(\mu_n)}\cdot A_n \qquad (6)$$

where:

$$A_n = C_1\cdot e^{-\mu_n^2\cdot\frac{a\tau}{R^2}}+(C_2-C_1)\cdot e^{-\mu_n^2\cdot\frac{a(\tau-\tau_1)}{R^2}}+\ldots$$

By inserting the corresponding value for $A_n$ into the relation (6), the following is obtained:

$$\sigma_z = \frac{\beta E}{1-\upsilon}\cdot\frac{v_i\cdot R^2}{8a}\left(1-\frac{2r^2}{R^2}\right)+$$
$$+\frac{\beta E}{1-\upsilon}\cdot\frac{R^2}{a}\sum_{n=1}^{\infty}\frac{2}{\mu_n^4}-\mu_n\frac{I_0\left(\mu_n\cdot\frac{r}{R}\right)}{I_1(\mu_n)}\cdot C_1\cdot e^{-\mu_n^2\cdot\frac{a\tau}{R^2}}+(C_2-C_1)\cdot e^{-\mu_n^2\cdot\frac{a(\tau-\tau_1)}{R^2}}+\ldots \qquad (7)$$

In order to perform the computations using the relation (7), one must take into account a large number of terms from infinite series. For the purpose of simplification, the relevant infinite series are approximated using the functions f $(\frac{a\tau}{R^2};\frac{r}{R})$. Thus, the relation (7) becomes:

$$\sigma_z = \frac{\beta E}{1-\upsilon}\cdot\frac{R^2}{a}\left\{\frac{v_i}{8}\left(1-\frac{2r^2}{R^2}\right)+C_1 f'+\left[(C_2-C_1)f''+(C_3-C_2)f'''+\ldots\right]\right\} \qquad (8)$$

where:
$v_i$ - represent the values of heating speed (i=1, 2, 3 …);

$C_p$, $\gamma$, $\lambda$, $\beta$, E, a ($a = \frac{\lambda}{C_p \gamma}$) – coefficients depending on the nature of the steel, having different values temperature variation. Their value is presented in Table 1.
The value of the inputted functions depends on the type of heating ($\tau$) and on the distance considered from the centre of the ingot to its surface (r).

Depending on the $\frac{r}{R}$ ratio and assigning different values to the time $\tau$, the value of the functions $f(\frac{a\tau}{R^2}; \frac{r}{R})$ at various distances from the centre of the ingot is obtained. The results are presented in Table 2, and for a more convenient use, based on these values, the nomogram in Figure 7 was traced, which indicates the value of the $f(\frac{a\tau}{R^2}; \frac{r}{R})$ functions for the heating of ingots made from the studied steel.
The calculation of thermal stresses is performed according to the type of heating throughout the entire surface of the ingot. As it can be observed from Table 2, compression stresses occur on the surface of the ingot, while at the centre of the ingot, tensile stresses.

Table 2. Value of the $f(\frac{a\tau}{R^2}; \frac{r}{R})$ functions and of the thermal stresses ($\sigma_z$) depending on the heating time ($\tau$) and on the distance from the centre of the ingot (r).

| Time | f | $\frac{r}{R}$ =1 | f | $\frac{r}{R}$ =0.8 | f | $\frac{r}{R}$ =0.6 | f | $\frac{r}{R}$ =0.4 | f | $\frac{r}{R}$ =0.2 | f | $\frac{r}{R}$ =0 |
|---|---|---|---|---|---|---|---|---|---|---|---|---|
| | | $\sigma_z$ N/mm² | | $\sigma_z$ N/mm² | | $\sigma_z$ N/mm² | | $\sigma_z$ N/mm² | | $\sigma_z$ N/mm² | | $\sigma_z$ N/mm² |
| 0.1 | 0.075 | -92.9 | 0.035 | -8.5 | -0.025 | -40.2 | 0.079 | 18.5 | 0.011 | 43.3 | -0.12 | 15.4 |
| 0.2 | 0.095 | -123.7 | 0.032 | -9.2 | -0.024 | -27.4 | 0.070 | 46.5 | 0.010 | 46.4 | -0.11 | 46.4 |
| 0.3 | 0.085 | -154.7 | 0.030 | -15.4 | -0.021 | -24.7 | 0.066 | 58.7 | 0.0097 | 47.3 | -0.10 | 77.3 |
| 0.4 | 0.080 | -233.1 | 0.027 | -24.7 | -0.020 | -18.4 | 0.060 | 77.3 | 0.0095 | 47.9 | -0.098 | 83.5 |
| 0.5 | 0.076 | -247.5 | 0.024 | -34.0 | -0.018 | -12.3 | 0.055 | 92.8 | 0.0078 | 53.2 | -0.097 | 117.5 |
| 0.6 | 0.072 | -278.5 | 0.021 | -43.3 | -0.016 | 0 | 0.047 | 108.3 | 0.0074 | 56.5 | -0.084 | 126.8 |
| 0.7 | 0.068 | -293.9 | 0.018 | -52.6 | -0.014 | 1.2 | 0.043 | 117.5 | 0.0068 | 56.7 | -0.080 | 139.2 |
| 0.8 | 0.065 | -309.4 | 0.015 | -61.8 | -0.012 | 2.7 | 0.039 | 129.9 | 0.0065 | 57.2 | -0.076 | 143.5 |
| 0.9 | 0.061 | -349.8 | 0.012 | -71.1 | -0.011 | 3 | 0.034 | 142.3 | 0.0061 | 58.4 | -0.071 | 151.6 |
| 1.0 | 0.057 | -356.0 | 0.008 | -83.5 | -0.007 | 15.4 | 0.030 | 157.8 | 0.0057 | 59.7 | -0.061 | 167.1 |

It is a known fact that tensile stresses are more dangerous than compressive stresses, because they often lead to the formation of cracks. For the determination of thermal stresses in circumstances in which the temperature of the furnace is changed in increments, we use the relation (8) where the parameters determined in Table 1 are inputted and, with the help of the nomogram in Figure 7, we can determine the value of the $f(\frac{a\tau}{R^2}; \frac{r}{R})$ functions.

By performing the calculation for different heating rates and for different temperatures, we obtain the value of thermal stresses presented in Table 3.

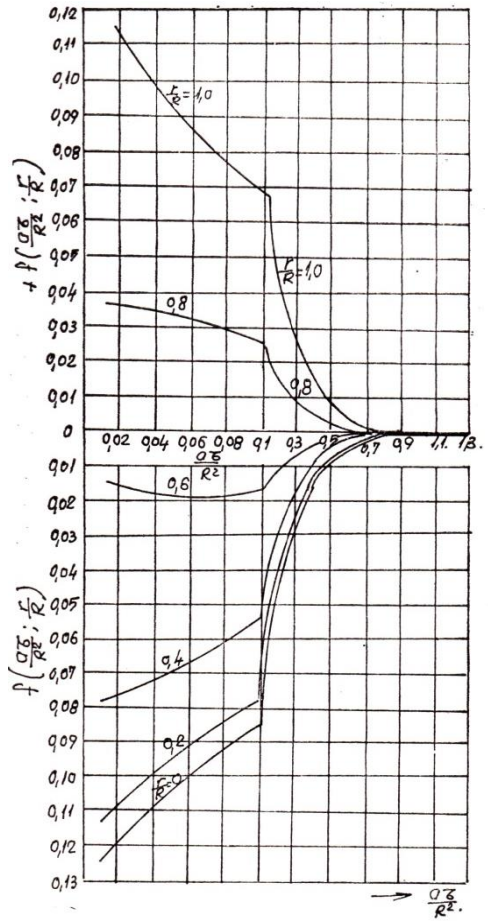

Fig. 7. Nomogram traced for function f ( $\frac{a\tau}{R^2}; \frac{r}{R}$ ) for determination of thermal stress in quality steel ingot [15]

Table 3. The value of thermal stresses depending on the heating rate and temperature

| $t_c$, °C / $v_i$ | 100 | 200 | 300 | 400 | 500 |
|---|---|---|---|---|---|
| The value of thermal stresses $\sigma_z$ N/mm$^2$ | | | | | |
| 54 | 110.0 | 139.5 | 131.4 | 114.1 | 92.7 |
| 79 | 160.9 | 200.0 | 191.5 | 163.3 | 135.7 |
| 100 | 203.7 | 257.5 | 242 | 211.2 | 171.2 |
| 150 | 305.6 | 386.3 | 360 | 316.6 | 250 |
| 180 | 366.7 | 460.0 | 432 | 380.2 | 308.2 |
| 200 | 404.7 | 515.0 | 485 | 423.4 | 340 |

If $\tau_n > 0.5\frac{R^2}{a}$, which corresponds to the practical case that is being analysed, the functions $f(\frac{a\tau}{R^2};\frac{r}{R})$ tend towards a minimum value (seeing that $\frac{a\tau}{R^2}$ becomes > 0.9) and can be neglected. This is due to the low thermal conductivity of 18-10 type steel, which at the sizes of the 3.6 t ingot (R ≈ 0.27 m), requires longer preheating times.

The calculation of thermal stresses in the case where the furnace temperature was changed in increments was performed when heating the experimental ingot within the 0-500 ºC range, applying six heating speeds (54, 79, 100, 150, 180 and 200ºC/h).

If one is to consider that the temperature of the ingot at the surface varies linearly, then the heating is achieved at the constant temperature $t_o$, the heating rate being uniform.

The temperature distribution on the ingot section under these heating conditions is given by the relation (9):

$$t = t_0 + C_\tau + \frac{CR^2}{4a}\left(\frac{r^2}{R^2} - 1\right) + \frac{CR^2}{a}\sum_{n=1}^{\infty}\frac{2}{\mu_n^3 I_1(\mu_n)} \cdot I_0\left(\mu_n \frac{r}{R}\right) e^{-\mu_n^2 \cdot \frac{a\tau}{R^2}} \tag{9}$$

Or, noting the sums of the infinite series $f(\frac{a\tau}{R^2};\frac{r}{R})$, the following is obtained:

$$t = t_0 + C_\tau + \frac{CR^2}{4a}\left(\frac{r^2}{R^2} - 1\right) + \frac{CR^2}{a} f\left(\frac{a\tau}{R^2}, \frac{r}{R}\right) \tag{10}$$

The starting point for determining the thermal stresses under conditions of linear temperature variation at the surface of the ingot is the relation (11):

$$\sigma_z = \varepsilon_z E + \frac{\beta E}{(1-\upsilon)}\left(-t + \frac{2\upsilon}{R^2}\int_0^R t_r d_r\right) \tag{11}$$

where $\varepsilon_z$ represents the axial deformation.

If the value of *t* is inputted into the relationship (11) and the integration is performed, the following is obtained:

$$\sigma_z = \frac{\beta E}{(1-\upsilon)} \cdot \frac{CR^2}{a}\left\{\frac{1}{8}\left(1 - \frac{2r^2}{R^2}\right) + \sum_{n=1}^{\infty}\frac{2}{\mu_n^4}\left[2 - \mu_n \frac{I_0\left(\mu_n \frac{r}{R}\right)}{I_1 \mu_n}\right] \cdot e^{-\mu_n^2 \cdot \frac{a\tau}{R^2}}\right\} \tag{12}$$

When replacing the infinite series with the $f(\frac{a\tau}{R^2};\frac{r}{R})$ functions we obtain the computation relation of thermal stresses in the analysed case:

$$\sigma_z = \frac{\beta E}{1-\upsilon} \cdot \frac{CR^2}{a}\left[\frac{1}{8}\left(1 - \frac{2r^2}{R^2}\right) + f(\frac{a\tau}{R^2};\frac{r}{R})\right] \tag{13}$$

In this case as well, the value of the parameters in the relation (13) is established analogously with the previous variant.
By performing the computation for the same heating rates and temperatures, we obtain the stresses presented in Table 4.

Table 4. The value of thermal stresses depending on the heating rate and temperature, when the ingot's ingot varies linearly

| $t_c$, °C / $v_i$ | 100 | 200 | 300 | 400 | 500 |
|---|---|---|---|---|---|
| The value of thermal stresses $\sigma_z$, N/mm$^2$ | | | | | |
| 54 | 137 | 132 | 113 | 109 | 92.7 |
| 79 | 204 | 191 | 161.5 | 159.2 | 132.5 |
| 100 | 250.2 | 241.2 | 209 | 197.1 | 175.9 |
| 150 | 376.2 | 332.1 | 324.2 | 301.1 | 235.4 |
| 180 | 441.9 | 418.9 | 374.2 | 353.9 | 307.8 |
| 200 | 545.1 | 502.5 | 420.2 | 384.4 | 362.7 |

Table 5 shows the value of the thermal stresses resulted at heating rates of 54, 79 and 100 °C/h respectively, taking into consideration the maximum temperature difference on the section of the ingot ($\Delta t_m$).
The thermal stresses resulted from the three analysed methods, depending on the heating rate applied by way of experiment, are graphically displayed in Figure 8.
In the third case, when the temperature difference on the section of the ingot is known by way of experiment, the thermal stresses can be calculated to an extent as close to reality as possible.
The temperature difference ($\Delta t_m$) can be determined analytically as well, with the relation:

$$(\Delta t_m) = \frac{CR^2}{4a} \tag{14}$$

By inputting the temperature difference $\Delta t_m$ in the relation (13) we obtain the calculation formula for thermal stresses in this case:

$$\sigma_z = \frac{\beta E}{1-\upsilon} \cdot \frac{CR^2}{8a}\left(1-\frac{2r^2}{R^2}\right) = \frac{\beta E}{1-\upsilon} \cdot \frac{\Delta t_m}{2}\left(1-\frac{2r^2}{R^2}\right) \tag{15}$$

The relation (15) establishes the value of thermal stresses in any point on the section of the ingot. If the determination of stresses is performed for the centre of the ingot, then the relation (15) becomes:

$$\sigma_z = \frac{\beta E}{1-\upsilon} \cdot \frac{\Delta t_m}{2} \tag{16}$$

Comparing the results obtained with the help of the three methods for the calculation of thermal stresses, it can be observed that, when using the temperature difference on section ($\Delta t_m$), the values recorded are maximal, the method being simpler and certainly greater for technological calculations.

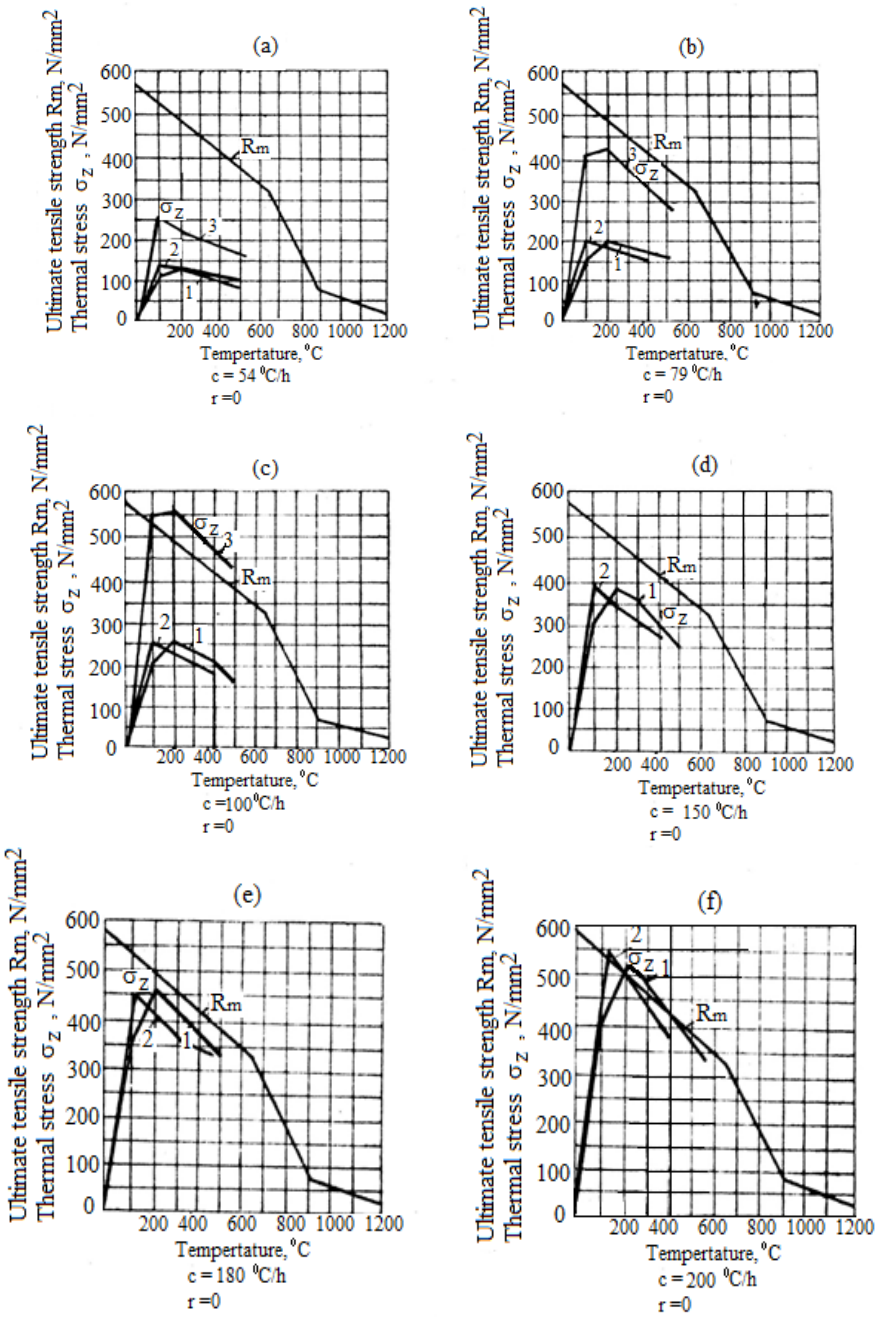


Fig. 8. Comparison between axial thermal stresses ($\sigma_z$) and the breaking strength ($R_m$), depending on the heating rate and temperature:
1 – thermal stresses when the furnace temperature is changed in increments; 2 – thermal stresses when the temperature at the surface of the ingot varies linearly; 3 – thermal stresses using the experimentally determined temperature difference on the ingot's surface.

## 3. Conclusions

The analysis of the research conducted domestically and abroad shows that the heating process for type 18-10 austenitic stainless steel raises some difficult issues and differs from one company to another, relying mostly on each company's own experience.

The paper determines the gradient and the thermal stresses depending on the heating rate, based on parameters resulted from industrial research, with a view to the optimisation of the process of heating austenitic stainless steel ingots, starting from the cold state.

The experimental variants have shown that lower values of the temperature difference on section, concurrently with the shortening of the heating time, can only be obtained by maintaining the furnace temperature at a constant value (approx. 600 ºC) after the cold ingots have been charged. The time period for obtaining the maximum value of the gradient is, in this case, of approx. 1 h, compared to 2 h, when the holding time was eliminated.

The optimal correspondence of results has allowed for the theoretical determination of the temperature value of the industrial furnace at the moment of charging the cold ingots, a value which guarantees a gradient lower to the critical value.

The axial thermal stresses $\sigma_z$, which occur up to the point when the temperature at the centre of the ingot does not exceed the perfect elasticity, compared with the breaking strength $R_m$, determined under hot-temperature conditions, prove that the currently applied technology can be improved.

The comparison of the results obtained using the three methods, graphically represented in Figure 8, reveals that, in case of using the temperature difference on section ($\Delta t_m$), we obtain maximum values.

This method takes into consideration to a greater extent the influence of the heating technology factors; it is simpler for technological calculations and has a better safety coefficient for the industrial practice.

The results of experimental research conducted on industrial aggregates, as well as the results of theoretical and laboratory research, have led to the creation of a technological process based on knowledge of the gradient and thermal stresses occurring on the section of the ingot during the heating at various speeds, on the influence of this process's dynamics on the structure and quality of products.

## References

[1] Z. Yanushkevich, A. Lugovskaya, A. Belyakov, R. Kaibyshev, *Deformation microstructures and tensile properties of an austenitic stainless steel subjected to multiple warm rolling*, Materials Science & Engineering A 667 (2016) 279–285

[2] Jun-xia HUANG, Xiao-ning YE, Zhou XU, *Effect of Cold Rolling on Microstructure and Mechanical Properties of AISI 301LN Metastable Austenitic Stainless Steels*, Journal of Iron and Steel Research, International ,Volume 19, Issue 10,(2012) 59-63

[3] Sumantra Mandal, P.V. Sivaprasad, S. Venugopal, K.P.N. Murthy, *Artificial neural network modeling to evaluate and predict the deformation behavior of stainless steel type AISI 304L during hot torsion*, Applied Soft Computing 9 (2009) 237–244
[4] M. Wendler, M. Hauser, O. Fabrichnaya, L. Krüger, A.Weiß, J. Mola, *Thermal and deformation-induced phase transformation behavior of Fe–15Cr–Mn–3Ni–0.1N–(0.05–0.25)C austenitic and austenitic – martensitic cast stainless steels*, Materials Science & Engineering A 645 (2015) 28-39
[5] YoungDeak Kim, JongRae Cho, WonByung Bae, *Efficient forging process to improve the closing effect of the inner void on an ultra-large ingot*, Journal of Materials Processing Technology 211 (2011) 1005–1013
[6] Suvi Papula, Severi Anttila, Juho Talonen, Teemu Sarikka, Iikka Virkkunen, Hannu Hänninen, *Strain hardening of cold-rolled lean-alloyed metastable ferritic-austenitic stainless steels*, Materials Science & Engineering A, 2016, http://dx.doi.org/10.1016/j.msea.2016.09.038
[7] Ilca I., Magaon J., *Structural research on semi–industrial high temperature stainless steel, thermostable*, VII International Congress, „Machinery, Technology, Materials" Sofia, Bulgaria, 2010
[8] Raţiu S., Alexa V., Ilca I., *Cercetarea deformabilităţii oţelurilor inoxidabile termostabile*, Conferinţa Naţională cu participare Internaţională, Ediţia a IV-a, Septembrie 2016, Cugir, România, pag. 109,
[9] Ilca I., *Tensiuni termice la încălzirea lingourilor din oţeluri de calitate în cuptoare industriale* „Materiale avansate, tratamente termice şi calitatea managementului", Academia de Ştiinţe Tehnice, Fil. Timişoara, 2001, 144
[10] Ilca I., Gaita D., Miloştean D., *Heating optimization of high grade steels for plastic processing*, A XVI-a Conferinţă internaţională - multidisciplinară „Profesorul Dorin Pavel – fondatorul hidroenergeticii româneşti", Sebeş, Ştiinţă şi Inginerie, Volumul 29-30/2016, 99-106
[11] Ioan ILCA, Imre KISS, Vasile ALEXA, Sorin Aurel RAŢIU, *Optimisation of the thermal treatment technologies for the cast hipereutectoid steel rolls*, Annals of Faculty Engineering Hunedoara – International Journal of Engineering, Tom XIV, Fascicula 3 (august), 2016, 201-206
[12] Tong Xi, Chunguang Yang, M. Babar Shahzad, Ke Yang, *Study of the processing map and hot deformation behavior of a Cu-bearing 317LN austenitic stainless steel*, Materials & Design, 87 (2015), 303–312
[13] Guixun Sun, Yu Zhang, Shicheng Sun, Jiangjiang Hu, Zhonghao Jiang, Changtao Ji, Jianshe Lian, *Plastic flow behavior and its relationship to tensile mechanical properties of high nitrogen nickel-free austenitic stainless steel, Materials Science and Engineering: A, Volume 662 (2016), 432–442*
[14] Catarschi V., Cucos I., Ioniţă I., Comaneci R., *Researches on the Heating Speed Influence on the Gradient and on Thermal Tension at the Alloy Steel Ingot Heating*, Lucrările primului Congres Internaţional de Ştiinţa şi Ingineria Materialelor, Iaşi, 1995, Buletinul Universităţii Tehnice din Iaşi, Tom XL, Vol. II, p. 980-985
[15] Taiţ N., Iu, *Tehnologhia nagreva stali*, Metelurghizdad, (1962), Moskova
[16] Samoilă C., Drugă L., Stan L., *Cuptoare şi instalaţii de încălzire*, Editura Tehnică, Bucureşti (1983)
[17] Ilca I., *The theory and practice of heating quality steel ingots*, Journal of Engineering Science Innovation, Volume 1, Issue 1 (2016), pp. 120-130